analytical chemistry

pubs.acs.org/ac Article

Free-Radical-Mediated Glycan Isomer Differentiation

Rayan Murtada,[§] Kimberly Fabijanczuk,[§] Kaylee Gaspar, Xueming Dong, Kawthar Zeyad Alzarieni, Kimberly Calix, Edgar Manriquez, Rose Mery Bakestani, Hilkka I. Kenttämaa, and Jinshan Gao*

Cite This: *Anal. Chem.* 2020, 92, 13794−13802 Read Online

ACCESS | Metrics & More | Article Recommendations | Supporting Information

ABSTRACT: The inherent structural complexity and diversity of glycans pose a major analytical challenge to their structural analysis. Radical chemistry has gained considerable momentum in the field of mass spectrometric biomolecule analysis, including proteomics, glycomics, and lipidomics. Herein, seven isomeric disaccharides and two isomeric tetrasaccharides with subtle structural differences are distinguished rapidly and accurately via one-step radical-induced dissociation. The free-radical-activated glycan-sequencing reagent (FRAGS) selectively conjugates to the unique reducing terminus of glycans in which a localized nascent free radical is generated upon collisional activation and simultaneously induces glycan fragmentation. Higher-energy collisional dissociation (HCD) and collision-induced dissociation (CID) are employed to provide complementary structural information for the identification and discrimination of glycan isomers by providing different fragmentation pathways to generate informative, structurally significant product ions. Furthermore, multiple-stage tandem mass spectrometry (MS^3 CID) provides supplementary and valuable structural information through the generation of characteristic parent-structure-dependent fragment ions.

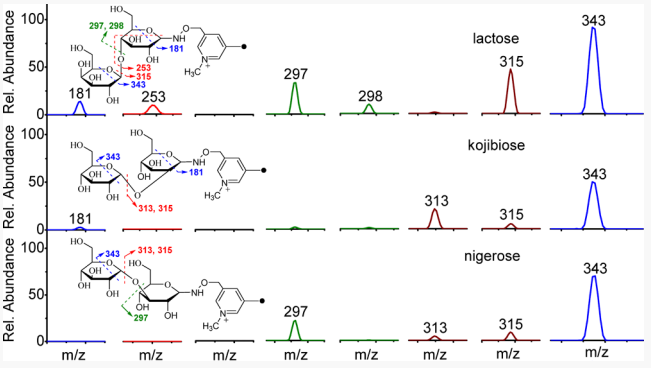

Glycans correspond to one of the four fundamental cellular macromolecules. The vast majority of glycans exhibit extremely complicated structures due to the diversity of linkage, anomeric configuration, stereocenters, and branches.[1] Unlike linear biopolymers, such as DNA, RNA, and gene-encoded proteins, that possess a limited number of subunits with a defined backbone consisting of phosphodiester or amide bonds, glycans are made by linking dozens of monosaccharide units together via complex regiochemical and stereochemical linkages.[2] The structures of glycans are described by the monosaccharide composition, types of connectivity, and entire configuration. Therefore, many constitutional isomers and stereoisomers exist. For instance, *D*-glucopyranose disaccharides formed by linking two glucose molecules can have 19 possible structures, with differences in the configuration of the glycosidic bond, such as kojibiose (α-1 → 2), nigerose (α-1 → 3), maltose (α-1 → 4), isomaltose (α-1 → 6), and cellobiose (β-1 → 4). Moreover, glycan epimers (including anomers that are epimers differing from each other at the anomeric center) are stereoisomers that differ in the configuration at only one stereocenter, even though the composition and connectivity are identical, such as cellobiose (β-D-glucopyranosyl-(1 → 4)-D-glucose) and lactose (β-D-galactopyranosyl-(1 → 4)-D-glucose) as well as isomaltose (α-D-glucopyranosyl-(1 → 6)-D-glucose) and melibiose (α-D-galactopyranosyl-(1 → 6)-D-glucose) (Figure 1). Therefore, the structural diversity of glycans is far more complicated than those of DNA, RNA, and proteins, making the discrimination of glycan isomers, especially epimers and anomers, quite challenging.

Many techniques, including high-performance liquid chromatography (HPLC),[3−5] ion mobility,[6−10] electrophoresis,[11,12] and nuclear magnetic resonance (NMR) spectroscopy,[13,14] have been employed for glycan structural analysis.[15] HPLC, electrophoresis, and ion mobility need well-characterized glycan standards, which are generally difficult to obtain in pure form. NMR requires relatively large quantities of a highly pure sample, which is time and cost consuming. Moreover, the interpretation of NMR spectra is difficult due to the similar chemical environments of many protons and carbons in glycans. Noted for multiple dissociation techniques, minimal sample consumption, short acquisition time, high sensitivity, high mass accuracy, and high resolution, mass spectrometry has been recognized as a powerful tool for glycan characterization and quantitation. Many mass spectrometric dissociation techniques have been demonstrated to provide complementary and extensive information for glycan structural analysis. Collision-induced dissociation[16−20] (CID) and infrared multi-

Received: May 24, 2020
Accepted: September 16, 2020
Published: September 16, 2020

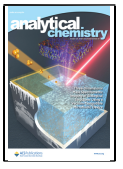

Downloaded via RUTGERS UNIV on February 5, 2021 at 15:50:49 (UTC).
See https://pubs.acs.org/sharingguidelines for options on how to legitimately share published articles.

© 2020 American Chemical Society

https://dx.doi.org/10.1021/acs.analchem.0c02213
Anal. Chem. 2020, 92, 13794−13802

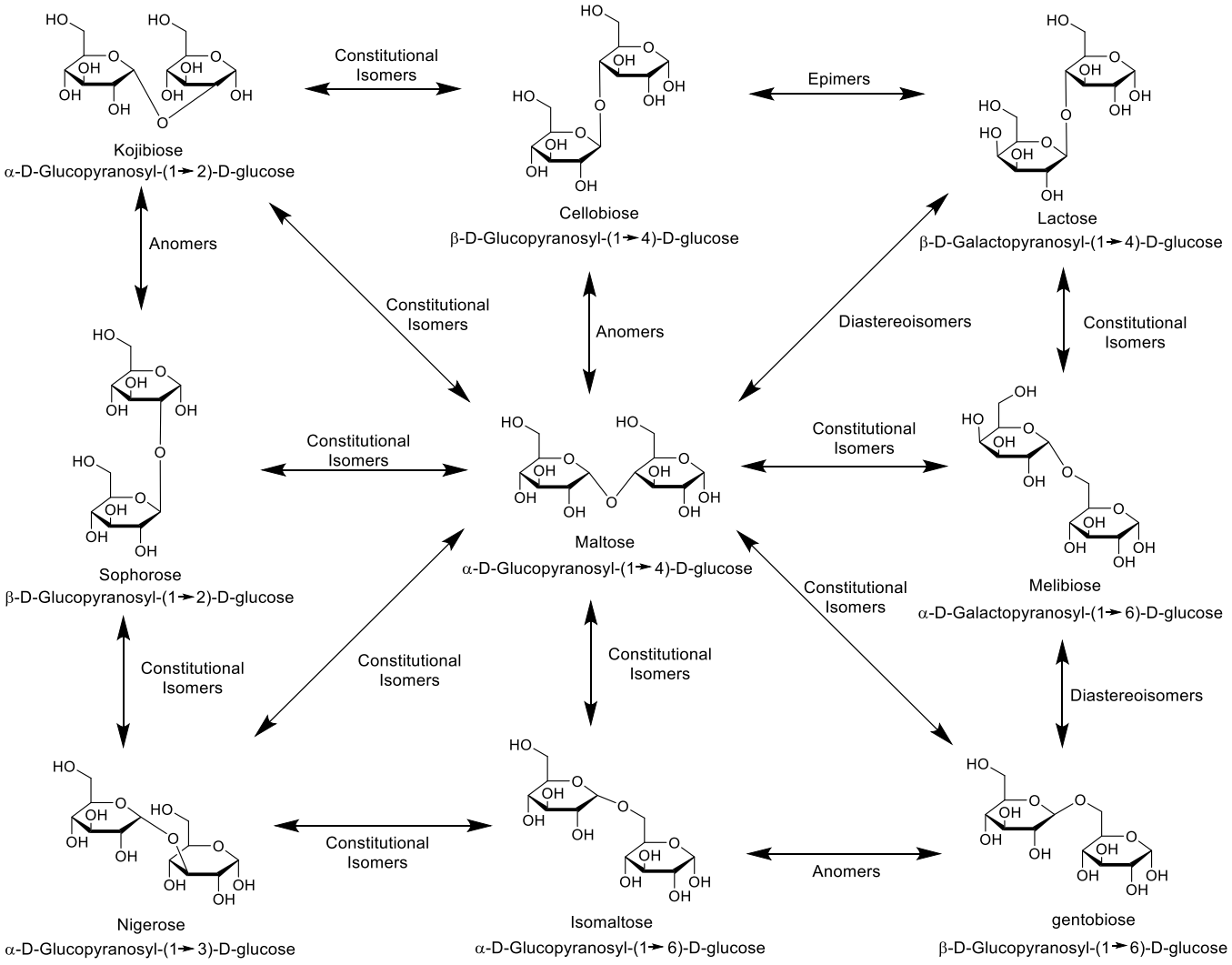

Figure 1. Representative disaccharides that differ in the linkage type, configuration, and composition.

photon dissociation[17,21] (IRMPD) typically generate glycosidic bond cleavages. Higher-energy collisional dissociation[22,23] (HCD) and ultraviolet photodissociation[24−26] (UVPD) have been demonstrated to generate more information-rich fragmentation patterns than those obtained by CID and IRMPD. Meanwhile, HCD has been demonstrated to yield multiple generations of product ions from multiple collisions and produce low-mass product ions for peptide/protein identification and quantitation.[27] Moreover, it has been proven that the fragmentation patterns and relative intensities of product ions upon collisional activation (CID or HCD) of protonated glycan isomers are nearly identical.[28,29] The low activation energy of the labile proton-catalyzed glycosidic bond dissociation is proposed to account for the similarity of fragmentation upon CID and HCD on protonated glycan isomers. Free-radical-driven dissociation techniques, including radical-directed dissociation (RDD),[28−30] electron capture dissociation (ECD),[17,31−34] electron transfer dissociation (ETD),[20,35−38] electron detachment dissociation (EDD),[39,40] and electronic excitation dissociation[5,41−43] (EED), have shown especially great promise for glycan structural characterization. In addition, free radical chemistry has also attracted significant attention in the field of proteomics[44−51] and lipidomics.[52−55] Although various mass spectrometric dissociation techniques have been applied to glycan structural elucidation, it is still challenging to differentiate stereoisomers, especially anomers and epimers. Tandem mass spectrometry,[56,57] ion-mobility mass spectrometry,[8] UVPD,[28] and EDD[43] have been developed for the differentiation of glycan isomers. For instance, linkage determination can be achieved by multiple-stage tandem mass spectrometry (MS^n) of derivatized glycans, metal-cationized disaccharides, and collision-induced dissociation (CID) of Z_1 ions in the negative ion mode.[18,56,57] The relatively low throughput of the MS^n approach hinders its application to online glycan separation. Ion-mobility, UVPD, and EDD have been limited to research groups equipped with these advanced instrumental capabilities. Recently, UVPD and EED have shown great potential for glycan isomer differentiation via the generation of characteristic free-radical-induced fragment ions. Inspired by the free-radical-driven dissociation techniques, we recently developed free-radical-activated glycan sequencing (FRAGS) reagents, which covalently and selectively add a free radical initiator on the reducing terminus of glycans.[29,58,59] This is an alternative method to generate a free radical at a well-defined site by collision-induced dissociation on FRAGS-derivatized glycans. In this study, we use a methylated free-radical-activated glycan sequencing reagent (Me-FRAGS), which combines a free

https://dx.doi.org/10.1021/acs.analchem.0c02213
Anal. Chem. 2020, 92, 13794−13802

radical precursor with a methylated pyridine moiety to provide a localized charge and therefore eradicate the misleading gas-phase glycan rearrangement.

EXPERIMENTAL SECTION

Glycans and Reagents. Maltose, cellobiose, lactose, melibiose, isomaltose, nigerose, kojibiose, sophorose, gentobiose, maltotetraose, and glucose tetrasaccharide were purchased from Sigma-Aldrich (St. Louis, MO, USA). All solvents were of HPLC grade and were purchased from EMD Merck (Gibbstown, NJ, USA). All other chemicals for the synthesis of Me-FRAGS reagent were purchased from Sigma-Aldrich (St. Louis, MO, USA). The synthesis of the Me-FRAGS reagent and the glycan derivatization were achieved according to previously reported procedures.[58] Me-FRAGS selectively couples with glycan epimers via derivatization at the unique reducing terminus in water in the presence of 10% acetic acid, which takes several hours at 50−70 °C. The introduction of the methyl group on the pyridine moiety was achieved by allowing the FRAGS-derivatized glycans to react with iodomethane in acetonitrile at room temperature for 6 h. The samples were dried via a vacuum concentrator and redissolved in 50/50 methanol/water (v/v).

Mass Spectrometry. Thermo-Fisher Scientific linear quadrupole ion trap (LTQ-XL) and LTQ-Orbitrap XL mass spectrometers (Thermo, San Jose, CA, USA) equipped with an electrospray ionization (ESI) source were employed. The bioconjugate sample solutions were directly infused into the ESI source of the mass spectrometer via a syringe pump at a flow rate of 5−10 μL/min. The critical parameters of the mass spectrometer include a spray voltage of 5−6 kV, a capillary voltage of 30−40 V, a capillary temperature of 250−275 °C, a sheath gas (N_2) flow rate of 10 (arbitrary unit), and a tube lens voltage of 50−200 V. Other ion optic parameters were optimized by the auto-tune function in the LTQ-XL tune program for maximizing the signal intensity. Higher-energy collisional dissociation (HCD) and collisional-induced dissociation (CID) on the ionized bioconjugates resulted in systematic glycan fragmentation processes and yielded characteristic ions depending on the structure of the glycan. The normalized HCD and CID energy was varied from 15 to 50 (arbitrary unit).

RESULTS AND DISCUSSION

All product ions are classified according to the Domon and Costello nomenclature (Figure 2).[41] To test the usefulness of the Me-FRAGS reagent for the differentiation of glycan isomers, we examined nine disaccharide isomers, maltose (*α-D-glucopyranosyl-(1 → 4)-D-glucose*), cellobiose (*β-D-glucopyranosyl-(1 → 4)-D-glucose*), lactose (*β-D-galactopyranosyl-(1 → 4)-D-glucose*), kojibiose (*α-D-glucopyranosyl-(1 → 2)-D-glucose*), sophorose (*β-D-glucopyranosyl-(1 → 2)-D-glucose*), nigerose (*α-D-glucopyranosyl-(1 → 3)-D-glucose*), isomaltose (*α-D-glucopyranosyl-(1 → 6)-D-glucose*), gentobiose (*β-D-glucopyranosyl-(1 → 6)-D-glucose*), melibiose (*α-D-galactopyranosyl-(1 → 6)-D-glucose*), and two tetrasaccharides, maltotetraose and glucose tetrasaccharide. Among these nine disaccharide isomers are pairs of anomers (epimers that differ in the configuration of the anomeric center): maltose and cellobiose, kojibiose and sophorose, and isomaltose and gentobiose. Cellobiose and lactose, as well as isomaltose and melibiose, are epimers, whereas maltose (α-1 → 4), nigerose (α-1 → 3), kojibiose (α-1 → 2), and isomaltose (α-1 → 6) are constitutional isomers differing only in the glycosidic linkage site but with the same configuration of the anomeric center.

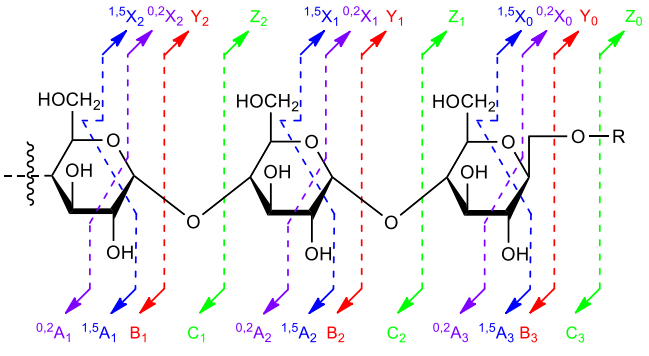

Figure 2. Nomenclature for glycan fragment ions.

Me-FRAGS selectively couples with glycan via derivatization at the unique reducing terminus, as shown in Scheme 1. The localized charge is used to avoid the misleading rearrangement ions, a common problem with slow-heating activation methods. A well-defined nascent free radical is generated at the radical precursor site (2,2,6,6-tetramethyl-1-piperidinyloxy, TEMPO) upon collisional activation and simultaneously induces systematic, predictable, and diagnostic cleavages. Glycan isomers, including anomers, epimers, and constitutional isomers, can be distinguished by simple one-step collisional activation. Not only do they differ in the relative intensity of product ions, but unique parent-structure-dependent product ions are also generated, as detailed below.

As shown in Figure 3, the fragmentation patterns and relative abundances of fragment ions upon CID of Me-FRAGS-derivatized nigerose are independent of the collision energy. There are no differences in the CID fragment ions and their relative abundances at normalized energies of 25, 35 and 45. No CID fragmentation was observed at a collision energy of 15. The most abundant fragment ions formed upon CID of Me-FRAGS-derivatized nigerose are Z_1, Y_1, and $^{1,5}X_1$. Interestingly, both the fragmentation patterns and the relative abundances of the fragment ions of FRGAS-derivatized nigerose vary with the change in the HCD collision energy. At the low HCD collision energy 15, only the precursor ion (*m/z* 632) and the ion corresponding to the loss of TEMPO are observed. At collision energy 25, the precursor ion remains visible, while ions formed upon elimination of TEMPO or (TEMPO+OH), as well as Z_1 and $^{1,5}X_1$ ions, dominate the spectrum. As the collision energy is ramped up to 35 and 45, not only do the precursor ions and ions formed via the loss of TEMPO completely fragment, but also the relative abundances of product ions change significantly. For instance, the relative abundances of the Z_1-H_2O ion (*m/z* 279), Y_1 + 2H ion (*m/z* 315), Z_1-$C_3H_6O_3$ ion (*m/z* 223), and $^{1,5}X_0$ + H ion (*m/z* 181) increase significantly. Moreover, new fragment ions appear, such as the $^{1,4}X_0$-CH_2O• ion (*m/z* 193) and the $^{1,4}X_0$-OH• ion (*m/z* 207). These additional ions serve as the glycans' "fingerprint", helping to confirm characteristics such as types of linkages, anomeric center configuration, and stereocenter, as detailed below. As the control, the CID and HCD of the nigerose sodium ion adduct were studied, wherein less fragmentation patterns were observed with ambiguous assignment without derivatization (Figure S1). Meanwhile, the CID and HCD of protonated derivatized glycan isomers generate

https://dx.doi.org/10.1021/acs.analchem.0c02213
Anal. Chem. 2020, 92, 13794−13802

Scheme 1. Diagram of Glycan Derivatization and Fragmentation upon One-Step HCD

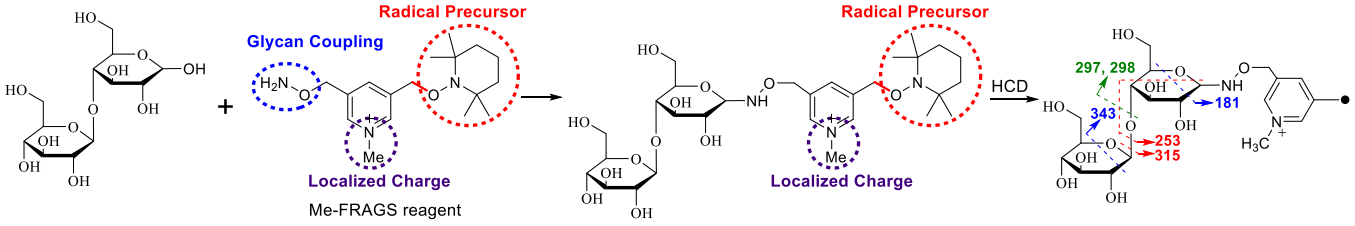

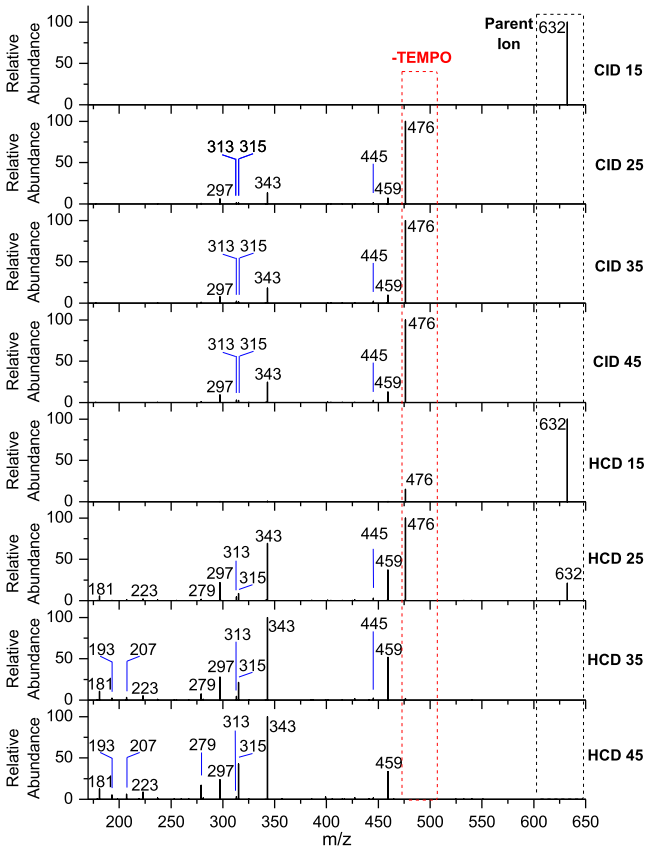

Figure 3. MS^2 spectra of Me-FRAGS-derivatized nigerose by CID and HCD with collisional energies of 15, 25, 35, and 45.

nearly identical fragmentation patterns and relative intensities of the product ions.[28,29] Therefore, the HCD of Me-FRAGS-derivatized nigerose can generate diverse informative fragment ions upon manipulation of the collision energy.

Not only are there differences in relative intensities of product ions, but also unique parent-structure-dependent product ions are generated upon HCD of Me-FRAGS-derivatized saccharide isomers. All nine isomers can be differentiated from each other by examining the zoomed-in fragment ions, as shown in Figure 4. The Y_1-$C_2H_4O_2$ ion (m/z 253) is a characteristic for disaccharides containing a 1−4 linkage, including maltose, cellobiose, and lactose. The relative abundance of the Y_1-$C_2H_4O_2$ ion increases with increasing the HCD energy from 20 to 35 (Figure S2−S5). The Y_1-$C_2H_4O_2$ ion is proposed to be formed by hydrogen atom abstraction from the C_2 site, β-elimination to form a double bond between C_1 and C_2 and an oxygen-centered radical, β-elimination to form a carbonyl group on C_5 and a carbon-centered radical on C_4, and finally β-elimination to form another carbonyl group on C_4 (Scheme 2). Moreover, the Y_1 + H-CH_2O (m/z 284) ion is unique for disaccharides with the 1−6 linkage including isomaltose, gentobiose, and melibiose, although the relative abundance is low, as shown in Figure 4. To further confirm that the Y + H-CH_2O ion is unique for 1−6 linkage glycans, Me-FRAGS-derivatized maltotetraose and glucose tetrasaccharide were subjected to collisional activation. Maltotetraose (Glcα1-4Glcα1-4Glcα1-4Glc) consists of four glucose subunits with identical α-1 → 4 linkages, whereas glucose tetrasaccharide (Glcα1-6Glcα1-4Glcα1-4Glc) consists of four glucose subunits with two α-1 → 4 and one terminal α-1 → 6 linkages. The collisional activation of Me-FRAGS-derivatized glucose tetrasaccharide generates a unique ion Y_3 + H-CH_2O (m/z 607) due to the presence of an α-1 → 6 linkage between the first and the second glucose unit from the nonreducing terminus (Figure S6). The formation of the Y_1 + H-CH_2O ion is proposed to be initiated by hydrogen atom abstraction from the C_2' site followed by two consecutive β-eliminations (Scheme 3).

As discussed above, the 1 → 4 linked isomers exhibit a parent-structure-dependent product ion Y_1-$C_2H_4O_2$, whereas the 1 → 6 linked isomers generate a Y_1 + H-CH_2O ion as the unique parent-structure-dependent product ion. Therefore, the nine isomeric disaccharides can be divided into three subgroups, 1 → 4 linked isomers, 1 → 6 linked isomers, and isomers with other linkages. Kojibiose and sophorose are 1 → 2 linked isomers, whereas nigerose is a 1 → 3 linked isomer. The HCD of Me-FRAGS-derivatized kojibiose and sophorose generates a quite different mass spectrum with respect to all other isomers. The relative abundances of Z_1 (m/z 297) and Z_1 + H (m/z 298) ions of these two isomers are much lower than those of all of the other isomers, which may be rationalized by the steric hindrance preventing the free radical from approaching the C_3 hydrogen. Moreover, kojibiose and sophorose are the only isomers that exhibit a higher abundance of the Y_1 ion (m/z 313) than the Y_1 + 2H ion (m/z 315) among the nine isomers at different HCD energy levels (Figure 4, Figures S2−S5). The Y_1 ion is formed by hydrogen abstraction from the C_1 site on the reducing terminal residue.[58] Meanwhile, the Y_1 + 2H ion is generated by hydrogen abstraction from the C_1' site on the nonreducing terminal residue.[58] R_{isomer} values, calculated using the following equation in which R_1 and R_2 refer to the abundance ratios of two selected pairs of MS^n fragment ions, have been used to quantify the differences between two MS^n spectra. The abundance ratio of fragment ions that differ most are generally used to differentiate isomers. A larger R_{isomer} value indicates a higher degree of differentiation. In the literature, an R_{isomer} threshold of >1.9 has been established for the differentiation of isomers subjected to CID fragmentation and >2.4 for the differentiation of isomers subjected to radical-directed dissociation (RDD).[28,60] The R_{isomer} values of the nine isomers at different HCD energy levels are summarized in Table 1 in which the R_{isomer} values vary with changing of the HCD energy levels

https://dx.doi.org/10.1021/acs.analchem.0c02213
Anal. Chem. 2020, 92, 13794−13802

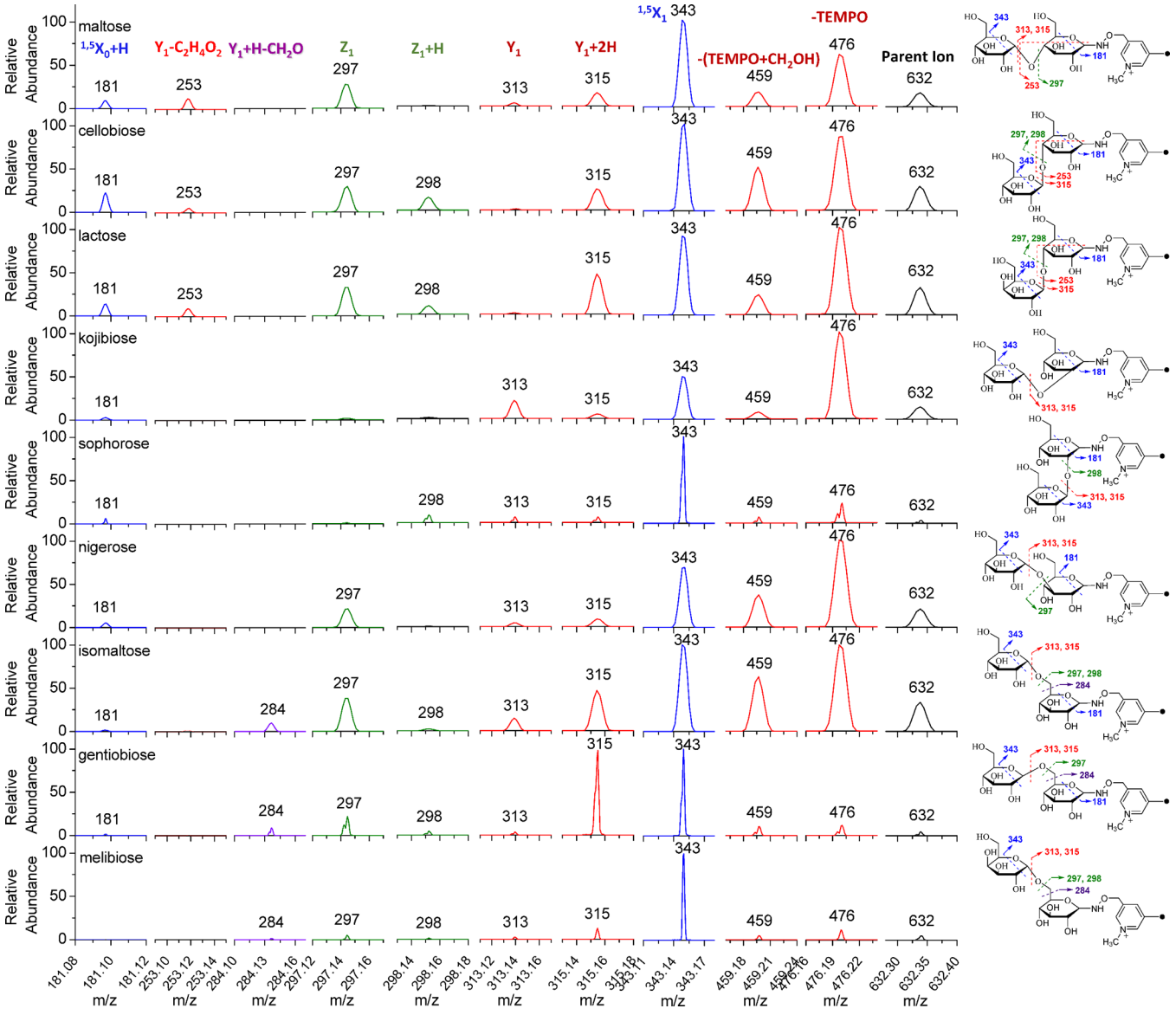

Figure 4. Zoomed-in MS^2 spectra of Me-FRAGS-derivatized disaccharides subjected to HCD with a collision energy of 25.

Scheme 2. Mechanism Proposed for the Formation of the Y_1-$C_2H_4O_2$ Ion

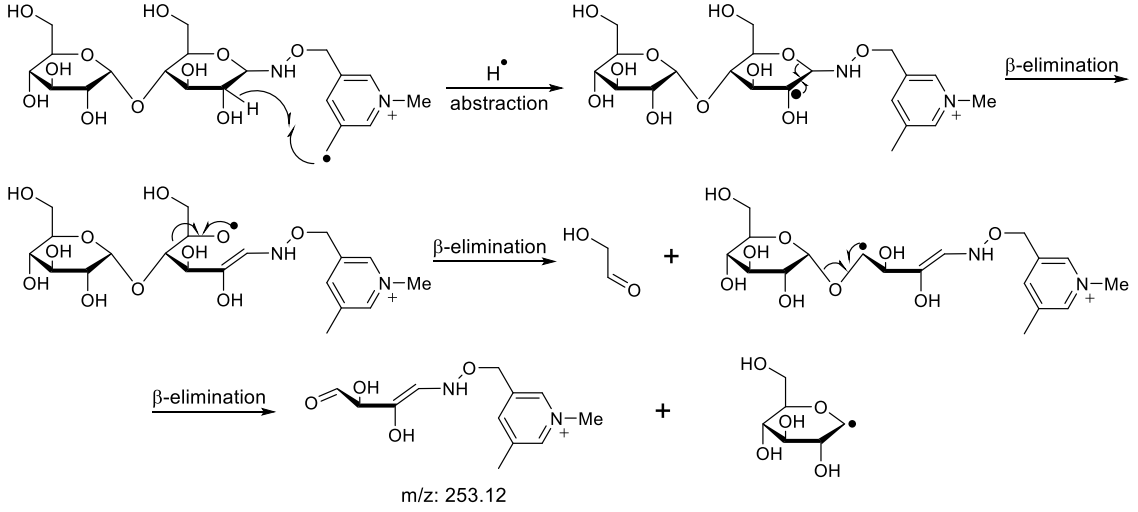

https://dx.doi.org/10.1021/acs.analchem.0c02213
Anal. Chem. 2020, 92, 13794−13802

Scheme 3. Mechanism Proposed for the Formation of the Y_1 + H-CH_2O Ion at the 1−6 Linkage Site

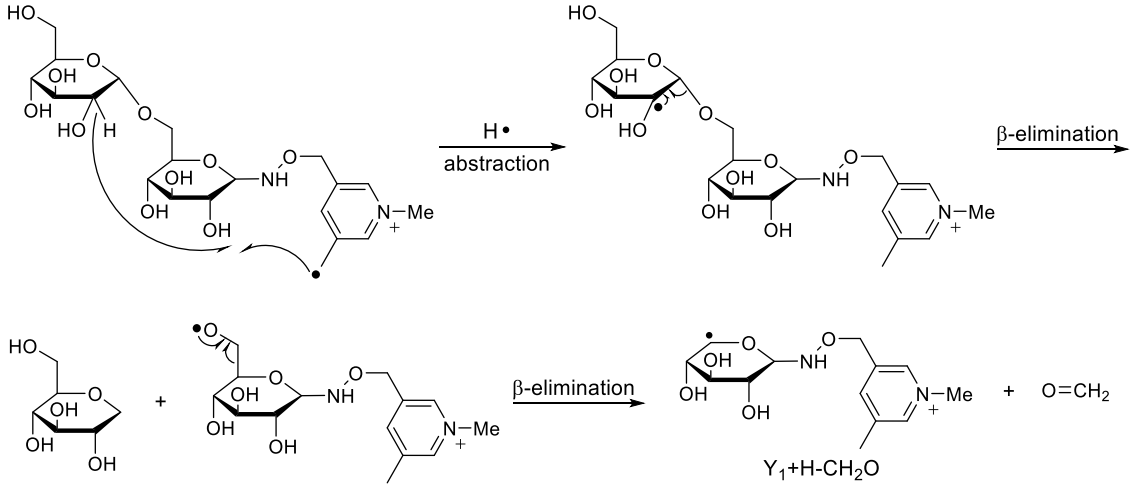

without a general trend for the variation. The R_{isomer} values at an HCD energy of 25 are mainly discussed. Nigerose can be distinguished from kojibiose by selecting *m/z* 297 and *m/z* 313 ions to obtain the R_{isomer} value of 52.3 at an HCD energy of 25 (Table 1), which is much larger than the R_{isomer} threshold, 2.4.

$$R_{isomer} = \frac{R_1}{R_2}$$

Differentiation between the diastereoisomers, anomers, and epimers, which differ only in the orientation of one and/or two bonds, is of the most difficult. For instance, lactose and cellobiose are epimers differing only in the orientation of the hydroxyl group on the C_4' site, maltose and cellobiose are anomers differing only in the orientation of the glycosidic bond, and maltose and lactose are diastereoisomers differing in the orientation of both the glycosidic bond and the hydroxyl group on the C_4' site. The abundance ratio of ions with *m/z* 253 and *m/z* 298 is inverted for maltose and lactose and maltose and cellobiose. The corresponding R_{isomer} values are 27.3 and 76.8, respectively (Table 1). Meanwhile, the abundance ratio of ions with *m/z* 315 and *m/z* 459 is inverted for cellobiose and lactose. This yields an R_{isomer} value of 4.07, which is much lower than the R_{isomer} values for the other two isomer pairs but still larger than the reported R_{isomer} threshold to identify isomers for radical-directed dissociation (RDD) fragmentation (R_{isomer} >2.4).[60] This can be rationalized by considering the structural differences among these three isomers. Cellobiose and lactose differ in only the orientation of the hydroxyl group on the C_4' site of the nonreducing terminal unit, which corresponds to the low R_{isomer} value. To further test the usefulness of the Me-FRAGS reagent for diastereoisomer, epimer, and anomer differentiation, three (1 → 6) linked isomers, somaltose, gentobiose, and melibiose, were selected. Isomaltose and gentobiose are anomers, isomaltose and melibiose are epimers, and gentobiose and melibiose are diastereoisomers. These three (1 → 6) linked isomers can be differentiated by R_{isomer} values ranging from 8.3 to 12.3 at an HCD energy of 25.

As discussed above, the HCD on the Me-FRAGS-derivatized glycans (MS^2) can be utilized to differentiate the nine isomeric disaccharides via characteristic parent-structure-dependent product ions and R_{isomer} values. To assess the ability of CID to differentiate glycan isomers, Me-FRAGS-derivatized disaccharides are subjected to collisional activation, wherein much fewer product ions are generated than those upon HCD due to the slow heating process, as shown in Figure S7. The Me-FRAGS CID spectra of the disaccharide isomers generate the same product ions with difference in the relative intensities of the fragment ions. The major fragment ions by CID are Z_1, Z_1 + H, Y_1, Y_1 + 2H,[1,5]X_1, TEMPO, and (TEMPO+CH_2OH). The linkage determination of disaccharides has been previously performed by multiple-stage tandem mass spectrometry (MS^n, n > 2) and collision-induced dissociation of Z_1 ions in the negative ion mode.[18] The MS^3 CID of the Z_1 ion generates distinct fragmentation fingerprints diagnostic for different linkage types. Therefore, MS^3 CID on different product ions was explored to test whether isomeric disaccharides can be distinguished based on characteristic MS^3 CID fragment ions. The results suggest that MS^3 CID on Z_1 ions (*m/z* 297) can be used to differentiate linkages based on the formation of characteristic fragment ions. An ion with *m/z* 223 is generated for disaccharides with a 1−6 linkage, an ion with *m/z* 279 is generated for disaccharides with a 1−4 linkage, ions with *m/z* 279 and 191 are generated for disaccharides with a 1−3 linkage, and ions with *m/z* 279, 237, and 223 ions are generated for disaccharides with a 1−2 linkage (Figure 5). It needs to be noted that MS^3 CID on the Z_1 ion of maltose also generates an *m/z* 223 ion, which can be used to differentiate it from its stereoisomers, cellobiose, and lactose. Therefore, CID provides complementary structural information to HCD. The generation of different fragmentation patterns for Z_1 ions upon CID can be rationalized by the structures of Z_1 ions formed for compounds with different linkages (Schemes S1−S4). MS^3 CID on other major MS^2 product ions, including Z_1 + H (*m/z* 298), Y_1 (*m/z* 313), Y_1 + 2H ions (*m/z* 315), and[1,5]X_1 (*m/z* 343), produces similar MS^3 product ions for all nine isomeric disaccharides.

■ CONCLUSIONS

Unique free-radical-induced parent-structure-dependent product ions are generated upon collisional dissociation (HCD and CID), which enables the confident, rapid, and accurate differentiation of glycan isomers with subtle structural differences. The Y_1-$C_2H_4O_2$ ion (*m/z* 253) is characteristic for disaccharides with a 1−4 linkage, including maltose, cellobiose, and lactose. The Y_1 + H-CH_2O ion is unique for

https://dx.doi.org/10.1021/acs.analchem.0c02213
Anal. Chem. 2020, 92, 13794−13802

Table 1. R_{isomer} Values

	isomer	cellobiose	lactose	kojibiose	sophorose	nigerose	isomaltose	gentobiose	melibiose
HCD 35	maltose	4.9 (181/253)	2.5 (181/253)	51.0 (181/313)	41.5 (207/315)	3.3 (181/459)	146.2 (181/313)	30.1 (181/315)	4.2 (297/343)
HCD 30		5.2 (181/253)	7.0 (313/315)	97.5 (297/313)	312.9 (207/297)	3.8 (181/459)	65.6 (181/313)	32.5 (181/315)	1.6 (297/343)
HCD 25		76.8 (253/298)	27.3 (253/298)	22.8 (181/313)	523.5 (297/298)	3.4 (343/459)	29.7 (181/313)	31.0 (181/315)	5.1 (297/343)
HCD 20		34.3 (298/343)	21.6 (298/343)	11.3 (313/343)	325.0 (297/298)	5.7 (343/459)	6.2 (315/343)	51.6 (315/476)	4.3 (343/476)
HCD 35	cellobiose		3.1 (315/459)	133.4 (181/313)	49.4 (207/459)	5.9 (181/297)	382.0 (181/313)	74.0 (181/315)	2.3 (343/459)
HCD 30			4.0 (315/459)	231.6 (181/313)	231.1 (207/297)	4.9 (181/297)	497.9 (181/313)	64.5 (181/315)	4.4 (343/459)
HCD 25			4.1 (315/459)	118.9 (313/459)	16.9 (297/298)	4.9 (181/476)	13.1 (298/315)	28.8 (315/476)	8.5 (298/343)
HCD 20			4.2 (315/459)	20.6 (298/476)	11.9 (297/476)	7.2 (315/476)	3.9 (298/343)	22.0 (315/476)	5.6 (343/476)
HCD 35	lactose			146.1 (181/313)	37.0 (207/315)	4.5 (181/459)	427.4 (181/313)	29.9 (181/315)	5.1 (297/343)
HCD 30				119.0 (313/315)	221.2 (207/297)	5.1 (181/459)	315.6 (181/313)	22.4 (181/315)	2.8 (315/343)
HCD 25				136.2 (313/315)	137.9 (297/313)	17.5 (313/315)	45.4 (298/313)	15.1 (181/315)	8.4 (343/476)
HCD 20				17.0 (315/476)	26.7 (297/298)	11.3 (315/476)	6.4 (298/459)	13.9 (315/476)	7.5 (343/476)
HCD 35	kojibiose				15.1 (207/313)	130.0 (297/313)	82.3 (181/297)	29.4 (313/315)	10.5 (313/343)
HCD 30					11.7 (207/313)	92.3 (297/313)	26.9 (297/313)	51.3 (313/315)	12.1 (313/343)
HCD 25					38.5 (298/476)	52.3 (297/313)	13.2 (313/315)	96.4 (313/315)	16.8 (343/476)
HCD 20					20.1 (298/476)	17.8 (313/459)	18.2 (313/315)	114.3 (313/315)	17.5 (343/476)
HCD 35	sophorose					64.6 (207/459)	65.3 (181/315)	60.4 (181/315)	4.6 (313/315)
HCD 30						385.5 (207/297)	78.5 (181/459)	54.5 (181/315)	43.4 (297/298)
HCD 25						39.7 (297/343)	156.7 (297/298)	14.5 (315/343)	25.7 (297/298)
HCD 20						345.2 (297/298)	56.9 (297/298)	34.9 (315/496)	6.0 (343/476)
HCD 35	nigerose						61.8 (181/313)	20.1 (181/315)	5.8 (297/343)
HCD 30							31.2 (181/313)	22.0 (315/459)	4.6 (343/459)
HCD 25							19.5 (181/315)	97.6 (315/476)	12.2 (343/476)
HCD 20							10.2 (315/476)	157.2 (315/476)	14.4 (343/476)
HCD 35	isomaltose							11.0 (315/459)	4.7 (343/459)
HCD 30								11.6 (315/459)	7.1 (343/459)
HCD 25								12.3 (315/459)	8.3 (343/476)
HCD 20								15.5 (315/476)	8.1 (343/476)
HCD 35	gentobiose								3.6 (313/459)
HCD 30									8.4 (315/459)
HCD 25									8.4 (315/343)
HCD 20									12.0 (315/343)

disaccharides with a 1−6 linkage. It is interesting that only 1 → 2 linked isomers, kojibiose and sophorose, produces a higher Y_1 ion than the Y_1 + 2H ion, while the other seven isomers yield higher Y_1 + 2H ion than the Y_1 ion. The differentiation of diastereoisomers, epimers, and anomers can be achieved using R_{isomer} obtained by comparing the abundance ratios of two pairs of fragment ions that differ the most in their relative abundances. For instance, cellobiose and lactose, differing in only the orientation of the hydroxyl group on the C_4' site, yield an R_{isomer} value of 4.07, which is still higher than the R_{isomer}

https://dx.doi.org/10.1021/acs.analchem.0c02213
Anal. Chem. 2020, 92, 13794−13802

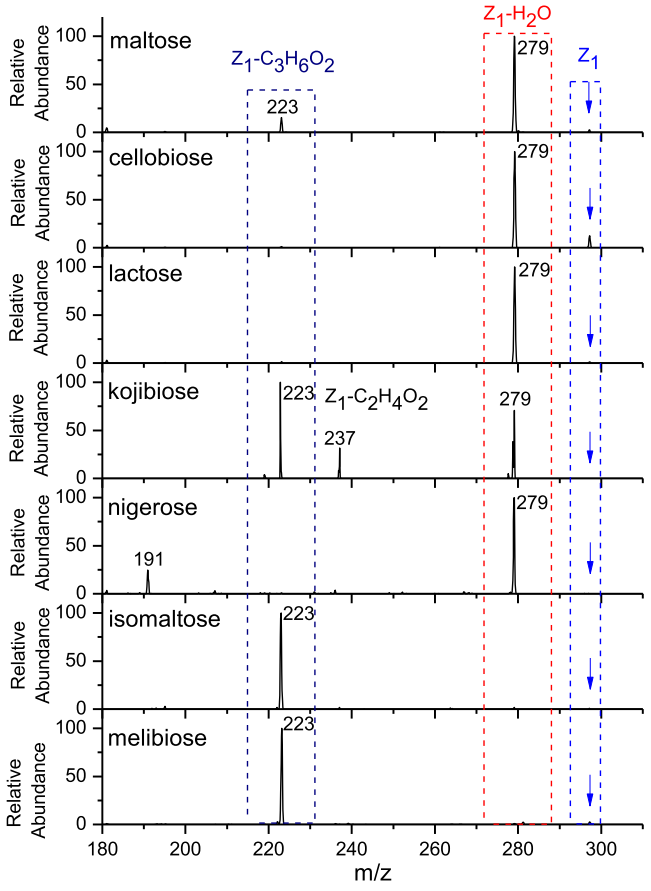

Figure 5. MS^3 CID spectra on Z_1 ions of disaccharides.

threshold to differentiate isomers by using radical-directed dissociation. Moreover, MS^3 CID on Z_1 ions generates characteristic fragment ions that enable the determination of the linkage type, including the *m/z* 223 ion diagnostic for compounds with a 1−6 linkage, the *m/z* 279 ion diagnostic for compounds with a 1−4 linkage, the *m/z* 279 and 191 ions diagnostic for compounds with a 1−3 linkage, and the *m/z* 279, 237, and 223 ions diagnostic for compounds with a 1−2 linkage. Therefore, the MS^3 CID significantly increases the confidence for the identification of the glycan isomers. The comprehensive fragmentation information from CID and HCD facilitates the structural characterization of isomeric glycans. Finally, the success in the differentiation of disaccharide isomers employing Me-FRAGS suggests its future application into large glycans especially when combined with HPLC/UPLC separation. Preliminary results support the feasibility of this approach.

■ ASSOCIATED CONTENT

Supporting Information

The Supporting Information is available free of charge at https://pubs.acs.org/doi/10.1021/acs.analchem.0c02213.

MS^2 spectra of Me-FRAGS-derivatized maltotetraose and glucose tetrasaccharide obtained using CID and HCD spectra of nine disaccharides at different energy levels (20, 25, 30, and 35); and proposed mechanisms for the formation of Z_1-H_2O, Z_1-$C_3H_6O_2$, and Z_1-$C_2H_4O_2$ ions (PDF)

■ AUTHOR INFORMATION

Corresponding Author

Jinshan Gao − *Department of Chemistry and Biochemistry, Montclair State University, Montclair, New Jersey 07043, United States;* orcid.org/0000-0001-9363-785X; Phone: 973-655-5136; Email: gaoj@montclair.edu; Fax: (+1)-973-655-7772

Authors

Rayan Murtada − *Department of Chemistry and Biochemistry, Montclair State University, Montclair, New Jersey 07043, United States*

Kimberly Fabijanczuk − *Department of Chemistry and Biochemistry, Montclair State University, Montclair, New Jersey 07043, United States*

Kaylee Gaspar − *Department of Chemistry and Biochemistry, Montclair State University, Montclair, New Jersey 07043, United States*

Xueming Dong − *Department of Chemistry, Purdue University, West Lafayette, Indiana 47907, United States*

Kawthar Zeyad Alzarieni − *Department of Chemistry, Purdue University, West Lafayette, Indiana 47907, United States*

Kimberly Calix − *Department of Chemistry and Biochemistry, Montclair State University, Montclair, New Jersey 07043, United States*

Edgar Manriquez − *Department of Chemistry and Biochemistry, Montclair State University, Montclair, New Jersey 07043, United States*

Rose Mery Bakestani − *Department of Chemistry and Biochemistry, Montclair State University, Montclair, New Jersey 07043, United States*

Hilkka I. Kenttämaa − *Department of Chemistry, Purdue University, West Lafayette, Indiana 47907, United States;* orcid.org/0000-0001-8988-6984

Complete contact information is available at: https://pubs.acs.org/10.1021/acs.analchem.0c02213

Author Contributions

§K.F. and R.M. have equal contribution.

Notes

The authors declare no competing financial interest.

■ ACKNOWLEDGMENTS

This work is supported by the National Science Foundation through grant CHEM1709272 and the National Institutes of Health through grant 1R15GM121986-01A1.

■ REFERENCES

(1) Council, N. R. *Transforming Glycoscience: A Roadmap for the Future* 2012.

(2) Varki, A.; Cummings, R. D.; Esko, J. D.; Stanley, P.; Hart, G. W.; Aebi, M.; Darvill, A. G.; Kinoshita, T.; Packer, N. H.; Prestegard, J. H.; Schnaar, R. L.; Seeberger, P. H., *Essentials of Glycobiology*, ThirdEdition. Cold Spring Harbor Laboratory Press, New York: 2017.

(3) Townsend, R. R.; Hardy, M. R.; Hindsgaul, O.; Lee, Y. C. *Anal. Biochem.* **1988**, *174*, 459−470.

(4) Jin, C.; Harvey, D. J.; Struwe, W. B.; Karlsson, N. G. *Anal. Chem.* **2019**, *91*, 10604−10613.

(5) Wei, J.; Tang, Y.; Bai, Y.; Zaia, J.; Costello, C. E.; Hong, P.; Lin, C. *Anal. Chem.* **2020**, *92*, 782−791.

(6) Harvey, D. J.; Scarff, C. A.; Crispin, M.; Scanlan, C. N.; Bonomelli, C.; Scrivens, J. H. *J. Am. Soc. Mass Spectrom.* **2012**, *23*, 1955−1966.

(7) Huang, Y.; Dodds, E. D. *Anal. Chem.* **2015**, *87*, 5664−5668.

(8) Hofmann, J.; Hahm, H. S.; Seeberger, P. H.; Pagel, K. *Nature* **2015**, *526*, 241−244.
(9) Warnke, S.; Ben Faleh, A.; Scutelnic, V.; Rizzo, T. R. *J. Am. Soc. Mass Spectrom.* **2019**, *30*, 2204−2211.
(10) Ben Faleh, A.; Warnke, S.; Rizzo, T. R. *Anal. Chem.* **2019**, *91*, 4876−4882.
(11) Hoffstetter-Kuhn, S.; Paulus, A.; Gassmann, E.; Widmer, H. M. *Anal. Chem.* **1991**, *63*, 1541−1547.
(12) Szabo, Z.; Guttman, A.; Rejtar, T.; Karger, B. L. *Electrophoresis* **2010**, *31*, 1389−1395.
(13) Fu, D.; Chen, L.; O'Neill, R. A. *Carbohydr. Res.* **1994**, *261*, 173−186.
(14) Szymanski, C. M.; Michael, F. S.; Jarrell, H. C.; Li, J.; Gilbert, M.; Larocque, S.; Vinogradov, E.; Brisson, J. R. *J. Biol. Chem.* **2003**, *278*, 24509−24520.
(15) Gray, C. J.; Migas, L. G.; Barran, P. E.; Pagel, K.; Seeberger, P. H.; Eyers, C. E.; Boons, G. J.; Pohl, N. L. B.; Compagnon, I.; Widmalm, G.; Flitsch, S. L. *J. Am. Chem. Soc.* **2019**, *141*, 14463−14479.
(16) Harvey, D. J. *J. Am. Soc. Mass Spectrom.* **2001**, *12*, 926−937.
(17) Adamson, J. T.; Håkansson, K. *Anal. Chem.* **2007**, *79*, 2901−2910.
(18) Konda, C.; Bendiak, B.; Xia, Y. *J. Am. Soc. Mass Spectrom.* **2014**, *25*, 248−257.
(19) Pellegrinelli, R. P.; Yue, L.; Carrascosa, E.; Warnke, S.; Ben Faleh, A.; Rizzo, T. R. *J. Am. Chem. Soc.* **2020**, *142*, 5948−5951.
(20) Schaller-Duke, R. M.; Bogala, M. R.; Cassady, C. J. *J. Am. Soc. Mass Spectrom.* **2018**, *29*, 1021−1035.
(21) Xie, Y.; Lebrilla, C. B. *Anal. Chem.* **2003**, *75*, 1590−1598.
(22) Harvey, D. J.; Bateman, R. H.; Green, M. R. *J. Mass Spectrom.* **1997**, *32*, 167−187.
(23) Yang, S.; Yuan, W.; Yang, W.; Zhou, J.; Harlan, R.; Edwards, J.; Li, S.; Zhang, H. *Anal. Chem.* **2013**, *85*, 8188−8195.
(24) Zhang, L.; Reilly, J. P. *J. Proteome Res.* **2009**, *8*, 734−742.
(25) Ko, B. J.; Brodbelt, J. S. *Anal. Chem.* **2011**, *83*, 8192−8200.
(26) Brodbelt, J. S. *Chem. Soc. Rev.* **2014**, *43*, 2757−2783.
(27) Diedrich, J. K.; Pinto, A. F. M.; Yates, J. R., 3rd *J. Am. Soc. Mass Spectrom.* **2013**, *24*, 1690−1699.
(28) Riggs, D. L.; Hofmann, J.; Hahm, H. S.; Seeberger, P. H.; Pagel, K.; Julian, R. R. *Anal. Chem.* **2018**, *90*, 11581−11588.
(29) Gao, J.; Thomas, D. A.; Sohn, C. H.; Beauchamp, J. L. *J. Am. Chem. Soc.* **2013**, *135*, 10684−10692.
(30) Zhang, X.; Julian, R. R. *Int. J. Mass Spectrom.* **2014**, *372*, 22−28.
(31) Budnik, B. A.; Haselmann, K. F.; Elkin, Y. N.; Gorbach, V. I.; Zubarev, R. A. *Anal. Chem.* **2003**, *75*, 5994−6001.
(32) Zhao, C.; Xie, B.; Chan, S.-Y.; Costello, C. E.; O'Connor, P. B. *J. Am. Soc. Mass Spectrom.* **2008**, *19*, 138−150.
(33) Huang, Y.; Pu, Y.; Yu, X.; Costello, C. E.; Lin, C. *J. Am. Soc. Mass Spectrom.* **2014**, *25*, 1451−1460.
(34) Yu, X.; Huang, Y.; Lin, C.; Costello, C. E. *Anal. Chem.* **2012**, *84*, 7487−7494.
(35) Leach, F. E.; Riley, N. M.; Westphall, M. S.; Coon, J. J.; Amster, I. J. *J. Am. Soc. Mass Spectrom.* **2017**, *28*, 1844−1854.
(36) Wolff, J. J.; Leach, F. E., III; Laremore, T. N.; Kaplan, D. A.; Easterling, M. L.; Linhardt, R. J.; Amster, I. J. *Anal. Chem.* **2010**, *82*, 3460−3466.
(37) Han, L.; Costello, C. E. *J. Am. Soc. Mass Spectrom.* **2011**, *22*, 997−1013.
(38) Wei, J.; Wu, J.; Tang, Y.; Ridgeway, M. E.; Park, M. A.; Costello, C. E.; Zaia, J.; Lin, C. *Anal. Chem.* **2019**, *91*, 2994−3001.
(39) Kornacki, J. R.; Adamson, J. T.; Håkansson, K. *J. Am. Soc. Mass Spectrom.* **2012**, *23*, 2031−2042.
(40) Kailemia, M. J.; Park, M.; Kaplan, D. A.; Venot, A.; Boons, G.-J.; Li, L.; Linhardt, R. J.; Amster, I. J. *J. Am. Soc. Mass Spectrom.* **2014**, *25*, 258−268.
(41) Yu, X.; Jiang, Y.; Chen, Y.; Huang, Y.; Costello, C. E.; Lin, C. *Anal. Chem.* **2013**, *85*, 10017−10021.
(42) Huang, Y.; Pu, Y.; Yu, X.; Costello, C. E.; Lin, C. *J. Am. Soc. Mass Spectrom.* **2016**, *27*, 319−328.
(43) Tang, Y.; Pu, Y.; Gao, J.; Hong, P.; Costello, C. E.; Lin, C. *Anal. Chem.* **2018**, *90*, 3793−3801.
(44) Hodyss, R.; Cox, H. A.; Beauchamp, J. L. *J. Am. Chem. Soc.* **2005**, *127*, 12436−12437.
(45) Thomas, D. A.; Sohn, C. H.; Gao, J.; Beauchamp, J. L. *J. Phys. Chem. A* **2014**, *118*, 8380−8392.
(46) Sohn, C. H.; Gao, J.; Thomas, D. A.; Kim, T.-Y.; Goddard, W. A., III; Beauchamp, J. L. *Chem. Sci.* **2015**, *6*, 4550−4560.
(47) Jang, I.; Lee, S. Y.; Hwangbo, S.; Kang, D.; Lee, H.; Kim, H. I.; Moon, B.; Oh, H. B. *J. Am. Soc. Mass Spectrom.* **2017**, *28*, 154−163.
(48) Masterson, D. S.; Yin, H.; Chacon, A.; Hachey, D. L.; Norris, J. L.; Porter, N. A. *J. Am. Chem. Soc.* **2004**, *126*, 720−721.
(49) Sun, Q.; Nelson, H.; Ly, T.; Stoltz, B. M.; Julian, R. R. *J. Proteome Res.* **2009**, *8*, 958−966.
(50) Tureček, F.; Julian, R. R. *Chem. Rev.* **2013**, *113*, 6691−6733.
(51) Gaspar, K.; Fabijanczuk, K.; Otegui, T.; Acosta, J.; Gao, J. *J. Am. Soc. Mass Spectrom.* **2019**, *30*, 548−556.
(52) Pham, H. T.; Julian, R. R. *Anal. Chem.* **2014**, *86*, 3020−3027.
(53) Pham, H. T.; Ly, T.; Trevitt, A. J.; Mitchell, T. W.; Blanksby, S. J. *Anal. Chem.* **2012**, *84*, 7525−7532.
(54) O'Brien, J. P.; Needham, B. D.; Henderson, J. C.; Nowicki, E. M.; Trent, M. S.; Brodbelt, J. S. *Anal. Chem.* **2014**, *86*, 2138−2145.
(55) Yin, H.; Xu, L.; Porter, N. A. *Chem. Rev.* **2011**, *111*, 5944−5972.
(56) Ashline, D. J.; Lapadula, A. J.; Liu, Y. H.; Lin, M.; Grace, M.; Pramanik, B.; Reinhold, V. N. *Anal. Chem.* **2007**, *79*, 3830−3842.
(57) Hofmeister, G. E.; Zhou, Z.; Leary, J. A. *J. Am. Chem. Soc.* **1991**, *113*, 5964−5970.
(58) Desai, N.; Thomas, D. A.; Lee, J.; Gao, J. S.; Beauchamp, J. L. *Chem. Sci.* **2016**, *7*, 5390−5397.
(59) Fabijanczuk, K.; Gaspar, K.; Desai, N.; Lee, J.; Thomas, D. A.; Beauchamp, J. L.; Gao, J. *Anal. Chem.* **2019**, *91*, 15387−15396.
(60) Tao, Y.; Julian, R. R. *Anal. Chem.* **2014**, *86*, 9733−9741.

https://dx.doi.org/10.1021/acs.analchem.0c02213
Anal. Chem. 2020, 92, 13794−13802